The role of reaction kinetics and mass transfer on the selective catalytic reduction of NO with NH_3 in monolithic reactors

Emilio Muñoz, Pablo Marín, Salvador Ordóñez*, Fernando V. Díez

Department of Chemical and Environmental Engineering, University of Oviedo, Facultad de Química, Julián Clavería 8, 33006 Oviedo, SPAIN

Abstract

Background

Environmental regulations are moving to a tighter control of NOx emissions produced at both stationary and mobile sources. Selective catalytic reduction (SCR) of NOx with NH_3 is an efficient treatment technique capable of operating at high gas flow rates (e.g. using monolithic catalysts) and a wide range of NO concentrations. The aim of this work is to provide guidelines for designing this kind of reactors taking into account both intrinsic kinetics and mass transfer.

Results

The experiments have been done in lab-scale (0.5 g) and bench-scale (430 g) reactors operating at different conditions: temperature (150-320ºC), space velocity (WHSV 5360-16100 mol h^{-1} kg_{cat}^{-1}), oxygen concentration (0-21%) and NH_3/NO ratio (0.2-1.2). Temperature has a great influence in the reaction rate, and at least 300ºC is required at a WHSV of 16100 mol h^{-1} kg_{cat}^{-1}. Oxygen is required in the feed because participates as reactant in the SCR.

Conclusions

Data obtained in the lab-scale reactor in the absence of mass transfer limitations have been used to fit an intrinsic kinetic model of the SCR reaction. A more complex model has been

used for the bench-scale reactor accounting for reaction kinetic and mass transfer (internal effectiveness factor was determined) in the monolithic catalyst.

Key words:

NOx emissions, air pollution control, monolithic catalyst, transient methods, mass transfer in monolithic reactors.

Notation

List of symbols

a	specific surface area ($m^2 \, m_{bed}^{-3}$)	
c	gas mole concentration (mol m^{-3})	
D_h	hydraulic diameter (m)	
D_{im}	mixture molecular diffusion coefficient ($m^2 \, s^{-1}$)	
D_{iz}	effective axial dispersion coefficient ($m^2 \, s^{-1}$)	
E_a	activation energy (J mol^{-1})	
k	kinetic constant ($m^3 \, mol^{-1} \, s^{-1}$ or s^{-1})	
K_g	mass transfer coefficient (m s^{-1})	
n	catalyst ammonia adsorption capacity (mol kg_{cat}^{-1})	
Q_g	gas flow rate ($m^3 \, s^{-1}$)	
r	reaction rate (mol $kg_{cat}^{-1} \, s^{-1}$)	
Sh	Sherwood number (-)	
t	time (s)	
T	temperature (K)	
t_{sw}	switching time (s)	
v	gas interstitial velocity (m s^{-1})	
w	relative weight of catalyst (-)	
W	total weight of catalyst (kg)	
z	spatial coordinate (m)	
	bed porosity (-)	
η_{int}	internal effectiveness factor	
θ	solid fraction of adsorbed specie (-)	
ρ_c	catalyst density (kg m^{-3})	

Sub indexes and super indexes

in   inlet

1   ads   adsorption
2   red   reduction
3   s   catalyst surface
4
5   *Acronyms*

6   BAT   best available techniques
7   FIC   flow indicator and controller
8   PI   pressure indicator
9   SCR   selective catalytic reduction
10 SNCR   selective non-catalytic reduction
11 TIC   temperature indicator and controller
12 WHSV   gas-hourly space velocity (mol h^{-1} kg$_{cat}^{-1}$)
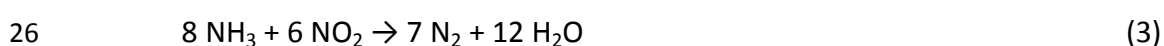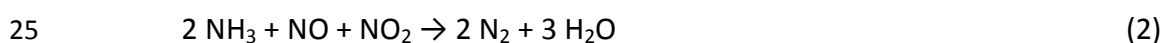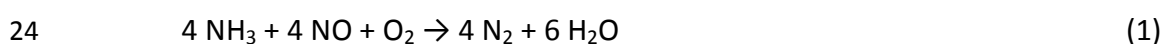13

14

15

1 Introduction

2 Nitric oxides (NO_x), including nitrogen oxide (NO), nitrogen dioxide (NO_2) and nitrous oxide

3 (N_2O), are emitted to the atmosphere mainly as a result of transportation and industrial

4 processes. They are among the most dangerous air pollutants, as they contribute to the

5 greenhouse effect, participate in photochemical reactions that cause acid rain and the

6 formation of troposphere ozone ('photochemical smog'), and have an important role in lakes

7 and rivers eutrophication. In addition, they are harmful to human health, as they can

8 damage the respiratory system.[1-3]

9 Due to their quantitative importance and harmful nature, NO_x abatement has been studied

10 widely during the last decades,[4-7] and their emissions in industrialized countries are

11 restrictively regulated, e.g. in the UE by Directive 2001/81/EC.

12 NO_x emissions can be reduced by means of primary or secondary measures. Primary

13 measures decrease NO_x formation, e.g. by controlling temperature, excess air or mixing in

14 combustion process, while secondary emissions separate or destroy NO_x from effluents.

15 Selective Catalytic Reduction (SCR) and Selective Non Catalytic Reduction (SNCR) are

16 secondary processes considered in the EU as Best Available Techniques (BAT) for treating

17 NO_x in emissions from large stationary sources, such as large combustion plants.[8] NO_x

18 selective reduction processes are based on the reaction of NO_x with a reducing agent

19 (ammonia or urea), forming molecular nitrogen and water. When performed in the presence

20 of a catalyst (SCR), the process takes place at lower temperature, is able of working with

21 load variations or variable fuel quality, and is substantially more efficient than when the

22 process is non-catalytic (SNCR). On the other hand, the inversion required for SNCR is lower.

23 The main reactions taking place for ammonia, the most common SCR reducing agent, are:

24
$$4\,NH_3 + 4\,NO + O_2 \rightarrow 4\,N_2 + 6\,H_2O \tag{1}$$

25
$$2\,NH_3 + NO + NO_2 \rightarrow 2\,N_2 + 3\,H_2O \tag{2}$$

26
$$8\,NH_3 + 6\,NO_2 \rightarrow 7\,N_2 + 12\,H_2O \tag{3}$$

Since NO/NO$_2$ ratio in NO$_x$ emissions is larger than 10, the first reaction, called 'standard SCR', is largely the most important. When temperature is low, the third reaction, called 'fast-SCR', should be also taken into consideration.

Different catalysts have been used for ammonia SCR, including noble metals, metal oxides and zeolites,[3, 9-11] operating temperature being an important factor for catalyst selection. For high temperatures (345-590ºC), zeolites are more durable, active and SO$_2$ tolerant.[12] Operating at lower temperature (typically 150-300ºC), allows saving fuel used for re-heating the flue gas in some installations. Noble metals have shown better performance at low temperature, but are expensive, the temperature operation range is narrow and present low sulphur tolerance. Pd and Ag are both noble metals that present good performance for the SCR reaction.[12, 13] Pd is usually supported on perovskites or zirconia. Ag supported on Al$_2$O$_3$ shows high efficiency, particularly when using hydrocarbons.

Metal oxide catalysts (oxides of copper, iron or vanadium, either unsupported or supported on alumina, silica or titania) [2, 8] are cheaper, and work well in the typical temperature range of industrial applications. One of the most common industrial SCR catalyst types consists on vanadium oxide, promoted by MoO$_3$ or WO$_3$, and supported on titania (in the anatase form). WO$_3$-V$_2$O$_5$/TiO$_2$ catalysts show tolerance to SO$_2$ poisoning and provide high NO$_x$ conversion, the TiO$_2$ support providing high surface area and increased catalyst activity.[8] In the last years, the research in this field has focused in the development of vanadium-free catalysts with high activity, selectivity and stability.[12, 13] Fe containing mixed oxides and Fe-exchanges zeolites were found to present high activity. The selection of an adequate support is critical for the activity and stability of the catalyst.[12, 14] Under rich oxygen conditions, Cu/ZSM-5 was found to present reduction capability using hydrocarbons.[13, 15]

SCR catalysts are generally used as structured beds, as this type of bed produces lower pressure drop through the reactor, helps to keep process conditions uniform along the bed, and presents higher resistance to attrition and lower tendency to fly ash plugging. A recent review about the catalyst and reactor configuration is presented by Cheng et al.[16]

Several mechanisms have been proposed for ammonia SCR on vanadia catalysts, including Langmuir-Hinsewood, Elay-Rideal and Mars Van Krevelen.[17-23] Most researchers have found that Elay-Rideal mechanisms fit better experimental results. Such models suppose that in
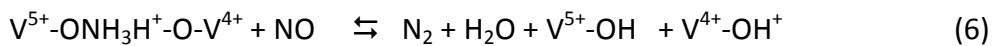
one step of the reaction mechanism, NO from the gas phase reacts with chemisorbed ammonia, but published works differ on the nature of the involved active sites and reaction intermediates.[24-26] Topsoe et al.[27, 28] observed in FTIR studies that, while at reaction conditions NO adsorbed is negligible, ammonia adsorbs in large amounts on both Lewis and Bronsted acid sites. Based on these studies, they proposed a mechanism according to which ammonia adsorbs in equilibrium on V^{5+}- OH sites:

$$NH_3 + V^{5+}\text{- OH} \leftrightarrows V^{5+}\text{- ONH}_4 \qquad (4)$$

Adsorbed ammonia is activated by adjacent $V^{5+}=O$ sites:

$$V^{5+}\text{-ONH}_4 + V^{5+}=O \leftrightarrows V^{5+}\text{-ONH}_3H^+\text{-O-V}^{4+} \qquad (5)$$
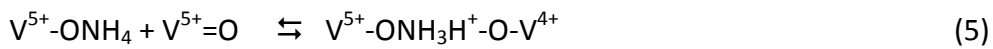
Activated ammonia reacts with NO:

$$V^{5+}\text{-ONH}_3H^+\text{-O-V}^{4+} + NO \leftrightarrows N_2 + H_2O + V^{5+}\text{-OH} + V^{4+}\text{-OH}^+ \qquad (6)$$

And finally, the active sites regenerate:

$$2\,V^{4+}\text{-OH}^+ \leftrightarrows H_2O + V^{3+} + V^{5+} \qquad (7)$$

$$O_2 + 2\,V^{3+} \leftrightarrows 2\,V^{5+}=O \qquad (8)$$

The kinetics of the ammonia SCR on vanadium catalysts has been widely studied in the literature, using equations either derived from reaction mechanisms or empirical.[22, 24, 26]

The aim of this work is to characterize the kinetics of ammonia SCR over a commercial monolithic metal oxide (vanadium on titania) catalyst, in order to get a comprehensive kinetic model adequate for simulating and optimizing the operation of steady and, specially, un-steady state SCR reactors. Firstly, a parametric study is carried out to determine the most important variables affecting the reaction kinetics. Then, an intrinsic kinetic model is proposed and fitted to lab-scale experiments. Finally, a model for the commercial monolith that takes into account the different mass transfer steps is tested and fitted to bench-scale experiments.

1 Methodology

2 Materials

3 High purity gaseous reactants (N_2, 2.5 % vol. NH_3 in nitrogen and 2.5 % vol. NO in nitrogen)
4 were provided by PRAXAIR, and air by a compressor provided with a filter to separate
5 humidity.

6 The catalyst used is a commercial DeNOx cordierite monolith, based on metal oxides, kindly
7 supplied by ARGILLON with square channels and 64 cpsi of cell density. The main
8 characteristics of the monolith, measured photographically, are: channel size $2.7 \ 10^{-3}$ m, wall
9 thickness $4.7 \ 10^{-4}$ m, washcoating thickness $9.6 \ 10^{-5}$ m. The bed porosity of the monolith
10 block was calculated to be 73%. The solid density of the catalyst was experimentally
11 determined to be 2500 kg m^{-3}.

12

13 Lab-scale fixed-bed reactor

14 The lab-scale fixed-bed reactor has been used to study the kinetics of the catalytic reaction
15 in absence of diffusional limitations, e.g. using the catalyst ground to a small particle size.
16 The reactor consists of a stainless steel tube of 9 mm inside diameter and 440 mm length. A
17 weight of 0.5 g of catalyst, ground and sieved to 250-355 μm, is mixed with 1 g of 355-710
18 μm glass particles and introduced inside the tube. The bed is set in position using stainless
19 steel foil. The geometry of this bed is adequate to minimize axial dispersion and channelling,
20 bed length/particle diameter = 54 > 50 and bed diameter/particle diameter = 30 > 10,
21 respectively. Hence, a gas flow pattern close to plug flow may be achieved inside the reactor.
22 Upstream the catalytic fixed-bed, the reactor tube is filled with 1 mm glass spheres to ensure
23 a uniform pre-heating of the gas feed. The reactor temperature was controlled by an electric
24 furnace and an electronic temperature controller that used the temperature measured by a
25 thermocouple placed inside the reactor as set point. The small reactor diameter and
26 catalytic bed length allowed assuming isothermal operation and negligible radial
27 temperature profiles.

28 The reactor feed is prepared by mixing streams from the ammonia and NO cylinders with air
29 or nitrogen in adequate proportions. The gas flow is measured and controlled by

1   BRONKHORST mass-flow controllers. The concentration of the reactor influent and effluent

2   are analysed using a quadrupole mass spectrometer, PFEIFFER VACUUM OMNISTAR. This

3   device is capable of analysing nitrogen monoxide and ammonia every few seconds. For each

4   experiment, the device is re-calibrated to ensure reliable quantitative measurements.

5

1   **Bench-scale fixed-bed reactor**

2   The bench-scale fixed-bed reactor allows the study of the reaction using the catalyst in the

3   commercial monolithic shape. The reactor consists of a stainless steel flanged tube of 57 mm

4   inside diameter and 450 mm length. A piece of monolith 250 mm long (430 g weight) was

5   cut to exactly fit inside the reactor. The monolith is maintained in place by means of a holey

6   stainless steel support. Upstream the monolith inside the reactor tube, a bed of 4 mm glass

7   spheres is used to obtain a feed of uniform temperature. The feed is heated up to the

8   operating temperature outside the reactor in an electrically-heated compact heat

9   exchanger. The temperature of the gas inside the reactor is measured before and after the

10 monolith. The reactor tube is housed in the middle of an electrically-heated furnace that is

11 responsible of achieving isothermal conditions. This is done by means of temperature

12 controllers that use the temperature measurements of the reactor inside to exert the

13 control action.

14 The preparation of the feed gas mixture and the analysis of the gases are carried out in the

15 same way as in the lab-scale reactor.

16 A scheme of the experimental units is shown in Figure 1.

17

18 **Modelling**

19 The aim of the modelling is to provide an appropriate model of the reactor capable of

20 predicting the dynamics of outlet concentrations. A 1D heterogeneous dynamic model has

21 been used. The model is heterogeneous, which means that accounts separately for the gas

22 and solid phases by means of the corresponding species mass balances. This allows the

23 prediction of the dynamics of the ammonia adsorbed on the catalyst.[29]

24 The model of the lab-scale fixed-bed reactor is shown in Table 1. This model is composed by

25 accumulation, convection and (intrinsic) reaction terms. The reaction mechanism assumed in

26 this work is a simplification of the one presented by Topsoe and Dumesic, in which only the

27 adsorption of ammonia and adsorbed ammonia reaction with NO are supposed to be

28 kinetically relevant (equations 4 and 6).[28, 29] Additionally, ammonia reaction with NO is

assumed to be irreversible. For the ammonia adsorption, a Temkin-type isotherm with zero activation energy is supposed. As explained in the previous section, the gas flow pattern of this reactor is close to plug flow, so no axial dispersion term is required. Moreover, the catalyst was ground to small particles, so that diffusion limitations can be neglected.

The bench-scale fixed-bed reactor is modelled with the same type of model, Table 2, formed by accumulation, convection, dispersion and mass transfer terms. In this case, the gas flow through the monolithic catalyst cannot be considered to follow a plug-flow pattern, so axial dispersion terms are included. Dispersion coefficients are calculated using a correlation specific for monolith catalysts,[30]   .

An issue that should be considered carefully in the modelling of monolithic catalysts is mass transfer. Gas to solid surface mass transfer is accounted for by means of the film theory using mass transfer coefficients,   , where Sherwood number,   , is 2.977 for square monolithic channels at isothermal conditions.[30] The specific surface is calculated from geometrical considerations using the hydraulic diameter of the monolith,   .
The interphase mass balances correlate gas to solid surface mass transfer and reaction terms. Additionally, mass transfer inside the monolith washcoating is modelled using internal effectiveness factor. This parameter, which depends on the textural properties of the washcoating, the intrinsic kinetics and the operating conditions, will be fitted to the experimental data.[31]

Both reactor models, lab-scale and bench-scale, are formed by a set of partial differential and algebraic equations. The models are solved by the 'method of lines', which consists of the approximation of the spatial derivatives (convection and dispersion terms) by finite differences in a grid of 400 points (this value was found to be high enough to obtain grid-independent solution). The resulting set of ordinary differential and algebraic equations is solved using the MATLAB function ode15s, especially suited for stiff problems. The whole problem is formulated in a code written in MATLAB.[32]

The fitting of model parameters has been done using the least-square technique, based on the minimization of the sum of the square residuals. The problem has been solved in MATLAB with the help of the lsqcurvefit function, using a trust-region-reflective algorithm.

Results and discussion

Parametric study of the SCR kinetics

The aim of this section is to conduct a systematic study of the main variables affecting the SCR reaction kinetics. Kinetic parameters have been measured by the transient response method.[4-6] The following variables were selected after preliminary works: temperature, oxygen concentration and NH_3/NO ratio.

Experiments consisted of measuring the evolution with time of the reactor effluent composition for different changes in the inlet composition, at constant flow rate and temperature. The experiments have been carried out in the lab-scale fixed-bed reactor described in the methodology section. Before all the experiments, the catalyst was saturated with ammonia at the corresponding temperature by flowing air with 500 ppm NH_3. At t = 0, this stream was substituted by the corresponding to each experiment.

Influence of temperature

Temperature is one of the main operating variables affecting the performance of the SCR reaction. This variable was studied by feeding to the reactor, with the catalyst previously saturated with ammonia, a stream containing of 500 ppm NO and NH_3 in air. The flow rate was 3 L min^{-1} n.t.p. (WHSV = 16100 mol h^{-1} kg$_{cat}^{-1}$) and experiments were isothermal in the temperature range 150-320ºC. After the transient, the new steady state was achieved in 3-4 min in all the tests. Figure 2 shows the transient of NO and NH_3 outlet concentrations.

The transient behaviour of NO and NH_3 outlet concentrations are strictly related to each other. Thus, the introduction of NO produces a marked peak in the measured NH_3 exit concentration. This can be caused by wrong signal from the mass detector when the inlet stream is changed, by NH_3 desorption from the catalyst, or by both. After the maximum, ammonia concentration goes down to the corresponding steady state value. NO concentration rises steadily at low temperatures (150-190ºC), whereas at high temperatures (220-320ºC) exhibits a small maximum before going down to the steady state value.

The influence of temperature in the steady state NO conversion can be examined in Figure 3a. Conversion is lower than 60% below 200ºC, so operation at these conditions is not interesting from an industrial point of view. For temperatures above 300ºC, the reaction of

1   NH$_3$ oxidation becomes important. This causes a reduction in NH$_3$ concentration and affects

2   NO conversion, which actually decreases at higher temperature, as reported elsewhere. [33, 34]

3

4   *Influence of oxygen concentration*

5   The role of oxygen is crucial in the SCR reaction, as it participates in the stoichiometric

6   equation as reactant, it is always present in these emissions, and it competes as oxidant

7   reactant with the NO. In the most accepted mechanism for this reaction, oxygen is

8   responsible of re-oxidizing the catalyst active sites.[21, 28] In this work, the effect of oxygen in

9   the performance of the reaction is assessed by varying the oxygen concentration (0, 0.08

10   and 0.21 mole fraction), while maintaining constant the other variables: 250ºC, inlet

11   concentrations 286 ppm NH$_3$, 500 ppm NO and balance nitrogen, and flow rate 2 L min^{-1}

12   n.t.p. (WHSV = 10700 mol h^{-1} kg$_{cat}^{-1}$). The transients for NO and NH$_3$ concentrations are

13   depicted in Figure 4. The steady state NO conversions obtained for the different oxygen

14   concentrations are shown in Figure 3b. This plot corroborates the role of oxygen in this

15   reaction.[35] When there is no oxygen in the feed, steady state conversion falls to zero, and at

16   conditions of excess oxygen (> 8 %), the concentration of oxygen does not affect steady state

17   NO conversion.

18   The unsteady state behaviour observed in this set of experiments is very useful to explain

19   the mechanism of this reaction. In all cases, NO concentration increases steadily up to the

20   steady state value, achieved after 8-10 minutes. The experiments with 8% and 21% oxygen

21   present similar behaviour with some differences. Thus, the presence of a higher oxygen

22   concentration delays the increase of NO outlet concentration. In the experiment with 8% of

23   oxygen, NH$_3$ exit concentration falls after the peak, which means a faster decrease in the

24   NH$_3$ catalyst surface coverage. It is well known that adsorbed NH$_3$ has a great impact on the

25   reaction rate.[10, 28] For this reason, the premature decrease in adsorbed NH$_3$ would cause the

26   observed increase on NO outlet concentration. It can be noted that for the test with 21% of

27   oxygen the amount of NO reacted and the amount of NH$_3$ desorbed (NH$_3$ spill) are both

28   higher than for the experiment with 8% of oxygen. This means that a higher amount of NH$_3$

29   was adsorbed during the saturation stage of the experiment with 21% of oxygen. More

30   adsorbed NH$_3$ means high NO conversion for more time and also a higher NH$_3$ spill.

As in the experiments of the previous section, when NO is fed to the reactor, a peak in NH_3 outlet concentration is observed, followed by a marked decrease. When no oxygen is fed to the reactor, the dynamics shown in Figure 4b is more complex, and can be explained based on the reaction mechanism. After the ammonia spill, reaction proceeds on the oxidized catalyst active sites, but the lack of oxygen in the gas phase avoids re-oxidation of the reduced catalyst active sites so, as the catalyst is depleted of oxidized active sites, the reaction rate decreases and eventually drops to 0 (NO concentration rises to the feed value, t = 4-6 min). However, the catalyst is still able of adsorbing NH_3 from the gas phase, causing the observed decrease in the NH_3 outlet concentration (t = 2-5 min). Finally, when the catalyst is saturated, NH_3 exit concentration increases again up to the feed value (t > 6 min). The dynamics of NH_3 concentration for the experiments with 0% and 21% of oxygen are similar, but as explained the consequences of this behaviour are different. At 21% oxygen, NH_3 is reacting with NO, whereas at 0% oxygen is adsorbing in the catalyst.

Influence of NH_3/NO ratio

The NH_3/NO ratio is an important operating variable in industrial scale reactors, which must be adjusted carefully to avoid slips of un-reacted NH_3. The stoichiometric NH_3/NO ratio for the SCR reaction is 1, but depending on the operating conditions, higher ratios can be used to compensate the loss of NH_3 by oxidation and other side reactions. The influence of the NH_3/NO ratio has been studied in the range 0.3-1.2 at different operating conditions: 250-300ºC and 1-2 L min^{-1} n.t.p. (WHSV = 5360-10700 mol h^{-1} kg_{cat}^{-1}).

As an illustration, Figure 5 shows the transient of a set of experiments, where NO feed concentration is kept constant at 500 ppm and NH_3 feed concentration is increased step-wise from 0 to 500 ppm. Hence, NH_3 is the limiting reactant, outlet NH_3 concentration being close to zero during the whole test. On the contrary, NO concentration decreases as NH_3 concentration increases, to reaction completion. The corresponding steady state NO conversions are depicted in Figure 3c for different operating conditions. The maximum NO conversion calculated from the stoichiometry, assuming complete NO reaction is indicated by a straight line. Thus, for NH_3/NO ratios lower than 0.8 nearly the maximum attainable NO conversion is achieved. For higher ratios, NO conversion tends to be independent of the

NH$_3$/NO ratio and highly dependent on temperature: an increase of 14% in NO conversion is observed when temperature increases from 250 to 300ºC. The influence of space time is less marked, only a 3% increase in NO conversion is obtained when the space time is halved. This behaviour is in agreement when previous studies that reported a critical NH$_3$/NO ratio of 0.7.[35]

Kinetic modelling

The experiments carried out at different operating conditions (temperature, flow rate and concentration) have been used to characterize the kinetics of the SCR reaction. As indicated in the methodology section, the monolithic catalyst was ground and sieved to a small size, in order to eliminate the influence on the kinetics of the diffusional steps. In that section, a model for the lab-scale fixed reactor based on gas and solid phase mass balances was also presented. This model must be completed with the kinetic equations, as show in Table 1. The mechanism of the reaction suggests the form of the kinetic equations: NH$_3$ absorbs and desorbs in the catalyst active sites according to first order elementary steps (net adsorption rate,   ) and NO from the gas phase reacts with adsorbed NH$_3$ (   ). The kinetic constants are assumed to vary with temperature according to Arrhenius dependence. The corresponding equations are included in Table 1.

The model parameters are calculated by fitting the model to the results of two types of experiments. The first type consists of NH$_3$ dynamic adsorption and desorption experiments on the catalyst. These tests were carried by flowing 500 ppm of ammonia in nitrogen in the adsorption, or nitrogen in the desorption experiments, in the range 150-300ºC and 1-3 L min^{-1} n.t.p. (WHSV 5360-16100 mol h^{-1} kg$_{cat}^{-1}$). Figure 6 (symbols) shows typical experimental results obtained in this case at 1 and 3 L min^{-1} n.t.p. and 300ºC.

In the adsorption experiment, a step of NH$_3$ is fed to the reactor and a breakthrough curve is obtained in the effluent. The existence of this sigmoidal breakthrough curve, instead of a straight step, indicates that the adsorption is not instantaneous, and hence equilibrium is only achieved at the end of the experiment, when the catalyst is completely saturated with NH$_3$. On increasing the gas flow rate, the transient of the experiment is modified, producing a decrease in the breakthrough time. Desorption experiments were carried out after the adsorption, when the NH$_3$ of the feed was replaced by nitrogen. This leads to the desorption

of most of the NH_3 previously adsorbed. Part of the NH_3 is adsorbed strongly, and can be desorbed only at higher temperature. The shape of the effluent concentration curve depends on the desorption reaction rate.

The dynamic NH_3 adsorption and desorption experiments allow the determination of the kinetic parameters of the net adsorption rate equation, e.g. adsorption and desorption kinetic constants (and   ) and total adsorption capacity (   ). These parameters have been obtained by fitting the un-steady state NH_3 outlet concentration predicted by the lab-scale fixed-bed reactor model to all the experimental data (adsorption and desorption) at once. It should be noted that in the model considered, adsorption and desorption curves are affected by both adsorption and desorption kinetic constants. Results are summarized in Table 3. Model predictions are depicted in Figure 6 (lines) together with the experimental data, in order to evaluate the goodness of the fitting. As shown, the model is able to predict the breakpoint of the adsorption tests accurately, small discrepancies being observed in the vicinity of the saturation.

The second type of experiments consists of NO reduction studies, in which NO and NH_3 are fed to the reactor, containing the catalyst previously saturated with NH_3. Experiments have been done at the following range of operating conditions: 220-320ºC, 1-3 L min^{-1} n.t.p. (WHSV 5360-16100 mol h^{-1} kg_{cat}^{-1}) and 500 ppm NO and 290-500 ppm NH_3. The unsteady state NO and NH_3 outlet concentrations are compared for experiments at 1 L min^{-1} n.t.p., 500 ppm NO and NH_3 and different temperatures in Figure 7. At the beginning of the experiment, NO conversion is complete because of the high reaction rate achieved when the catalyst is saturated with NH_3. As the reduction reaction proceeds, adsorbed NH_3 decreases, which is only partially replaced by NH_3 from the gas phase, so reaction rate decreases gradually (and hence NO concentration increases), until reaching the steady state.

The results of these experiments were used for fitting the kinetic parameters corresponding to the SCR reaction. As before, all the unsteady state concentration data have been used together in the fitting. The values used for the adsorption parameters were the ones determined in the adsorption experiments. Results can be found in Table 3.

1 Reactor modelling

2 The experiments carried out in the lab-scale fixed-bed reactor are useful to get insight into

3 the catalyst kinetics, but give no information on the influence of mass transfer processes in

4 the monolith. For this reason, additional experiments have been carried out in the bench-

5 scale fixed-bed reactor, in which the catalyst is used in its commercial monolithic shape.

6 Information obtained in this way represents better the behaviour of the catalyst in

7 industrial-scale reactors. The range of operating conditions in these experiments

8 corresponds to temperature 180-300ºC and flow rate 8-12 L min^{-1} n.t.p. (WHSV 35.6-53.4

9 mol kg$_{cat}^{-1}$ h^{-1}). NO and NH$_3$ feed concentrations have been fixed to 500 ppm.

10 As explained in the methodology section, external and internal mass transfer must be

11 accounted for in the model of the bench-scale reactor (see equations in Table 2). External

12 mass transfer in the monolithic channels was modelled using a literature correlation.[30] On

13 the contrary, internal mass transfer in the monolithic washcoating, modelled by the internal

14 effectiveness factor (   ), was fitted to the data obtained in this set of experiments. The

15 fitting has been done by least-square regression of the NO conversion obtained at steady-

16 state. This way, the risk of misleading internal mass transfer due to transient phenomena

17 (e.g. NH$_3$ adsorption and desorption dynamics) is eliminated.

18 For each experiment, the internal effectiveness factor that fits the experimental NO

19 conversion was determined. It was found that the internal effectiveness factors obtained

20 from experiments at the same temperature but different flow rates were not significantly

21 different. This is in agreement with a phenomenological analysis of internal mass transfer,

22 which suggests that the rate of mass transfer depends on the textural properties of the

23 washcoating, the physical properties of the gas (diffusion coefficients) and the intrinsic

24 kinetics. These properties may depend on temperature, but not on gas flow rate. Regarding

25 temperature, it was found that the internal effectiveness factor is highly influenced by this

26 parameter; an exponential decrease with temperature was observed. Thus, the data were fit

27 to the following expression, found to provide the best fit: . The

28 goodness of the fitting can be observed in Figure 8; the correlation coefficient R^2 was 0.993.

29 The performance of the reactor model, completed with the internal effectiveness factor, was

30 tested at steady and unsteady state conditions by comparison with experimental data. In

Figure 9, the steady state NO conversion used to calculate the internal effectiveness factors (symbols) are depicted together with the predictions of the reactor model (line). It can be observed that the model is able to predict the experimental data successfully within the temperature range considered.

The performance of the model in unsteady state is evaluated in Figure 10 in terms of the evolution of NO concentration at the reactor exit. The conditions of the experiment, which influence the interpretation of the results, are the following: first, only NO is fed to the reactor and when the outlet concentration is constant, NH_3 is added in stoiquiometric proportion. For this reason, a transient decrease of NO is observed, until the steady state value is reached. Figure 10 shows that the reactor model is able of predicting this transient in the temperature range considered in this work. As shown, on increasing temperature the decrease is more pronounced and the steady state is reached faster.

Conclusions

The kinetics of NO SCR has been studied in two fixed-bed reactors, a lab-scale reactor using ground catalyst and a bench-scale reactor using the catalyst in its commercial monolithic shape.

The parametric study of the reaction carried out with the most important variables has revealed the following conclusions. Temperature has a great influence in the reaction rate, and at least 300ºC is required at a WHSV of 16100 mol h^{-1} kg_{cat}^{-1}. Oxygen is required in the feed because participates as reactant in the SCR, having a positive effect on the reaction rate below 8% oxygen.

The experiments done at the lab-scale reactor have been used for the fitting of a kinetic model, based on a reaction mechanism considering the adsorption of NH_3 on the catalyst, followed by the reaction between NO and adsorbed NH_3 with satisfactory results.

Additional experiments carried out in the bench-scale reactor were used for the modelling of mass transfer in the monolithic catalyst. Thus, the internal effectiveness factor was calculated and correlated with temperature. Overall, the reactor model is able of predicting both steady and unsteady state experiments.

17

1

Acknowledgements

6

7

1

Caption to figures

3

4   Figure 1   Diagram of the bench-scale reactor.

5   Figure 2   Influence of temperature. Transient in NO (a) and NH$_3$ (b) outlet
6   concentrations. Flow rate = 3 L min^{-1} n.t.p. NO and NH$_3$ inlet concentration =
7   500 ppm. Temperature: 150ºC (——), 170ºC (— —), 190ºC (• ——), 220ºC (- -),
8   280ºC (• ——) and 320ºC (•••).

9   Figure 3   Steady state NO conversion. Influence of operating variables:
10   (a) Temperature. 3 L min^{-1} n.t.p., NH$_3$/NO=1.
11   (b) Oxygen concentration. 2 L min^{-1} n.t.p., 250ºC, NH$_3$/NO=0.6.
12   (c) NH$_3$/NO ratio. (■) 2 L min^{-1} n.t.p., 250ºC. (◆) 2 L min^{-1} n.t.p., 300ºC. (▲) 1
13   L min^{-1} n.t.p., 300ºC. The straight line indicates the maximum stoichiometric
14   NO conversion.

15   Figure 4   Influence of oxygen concentration. Transient in NO (a) and NH$_3$ (b) outlet
16   concentrations. Flow rate = 2 L min^{-1} n.t.p., temperature = 250ºC,
17   NH$_3$/NO=0.6. Oxygen concentration: 0% (——), 8% (— —) and 21% (- -).

18   Figure 5   Influence of NH$_3$/NO feed ratio. Variation of NH$_3$ feed concentration (•••) and
19   the corresponding evolution in NO (——) and NH$_3$ (— —) outlet concentrations.
20   Flow rate = 2 L min^{-1} n.t.p., temperature = 250ºC.

21   Figure 6   Fitting of NH$_3$ adsorption (a) and desorption (b) transient experiments. Feed
22   concentration: 500 ppm. Temperature: 300ºC. Flow rate: 1 (●) and 3 L min^{-1}
23   n.t.p. (▲). Symbols: experiments. Lines: model fitting.

24   Figure 7   Fitting of NO transient reduction experiments: NO (a) and NH$_3$ (b) effluent
25   concentrations. Feed concentration: 500 ppm NO and NH$_3$. Flow rate: 1 L min^{-}
26   ^{1} n.t.p. Temperature: 220 (◆), 280 (▲) and 320ºC (●). Symbols: experiments.
27   Lines: model fitting.

1   Figure 8   Influence of temperature in the internal effectiveness factor. Symbols:
2   internal effectiveness factor fit from experiments. Line: fitting.

3   Figure 9   Comparison of model simulations (line) and experiments (symbols) in terms of
4   NO steady state conversion. Flow rate: 8-12 L min^{-1} n.t.p. Inlet concentration:
5   500 ppm NO and NH_3.

6   Figure 10   Evaluation of the performance of the model to predict the unsteady state
7   experiments in the bench scale reactor. Flow rate: 8 L min^{-1} n.t.p.
8   Concentrations: 500 ppm NO and NH_3. Temperature: 180 (◆), 250 (▲) and
9   300ºC (●). Symbols: experiments. Lines: simulations.

10

11

1

2 **Figure 1**

3
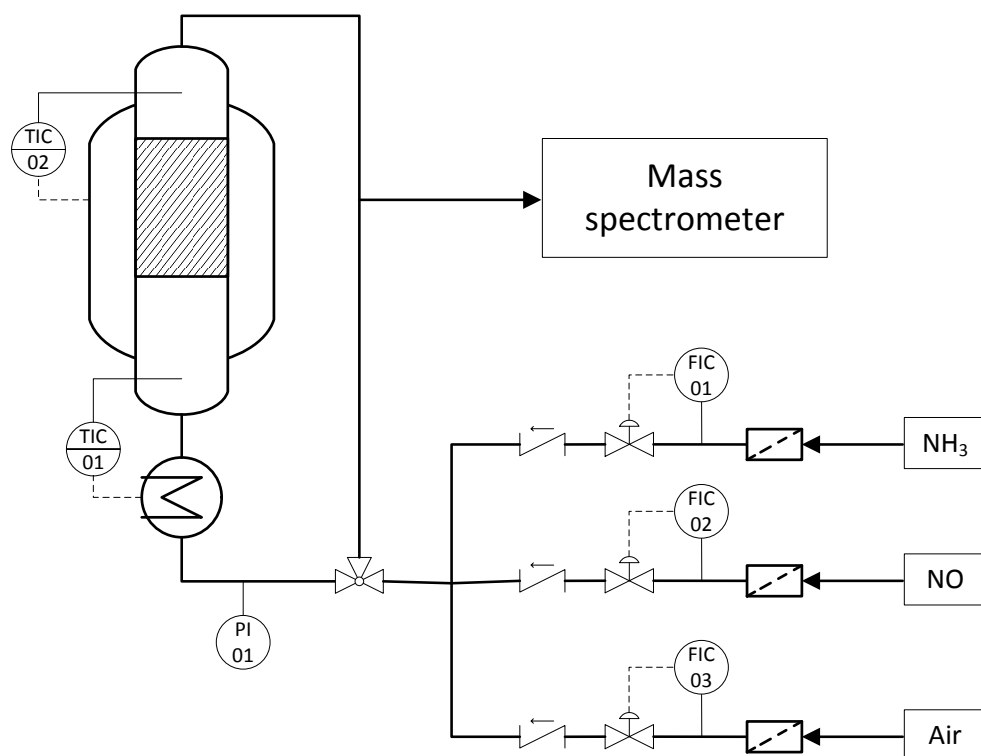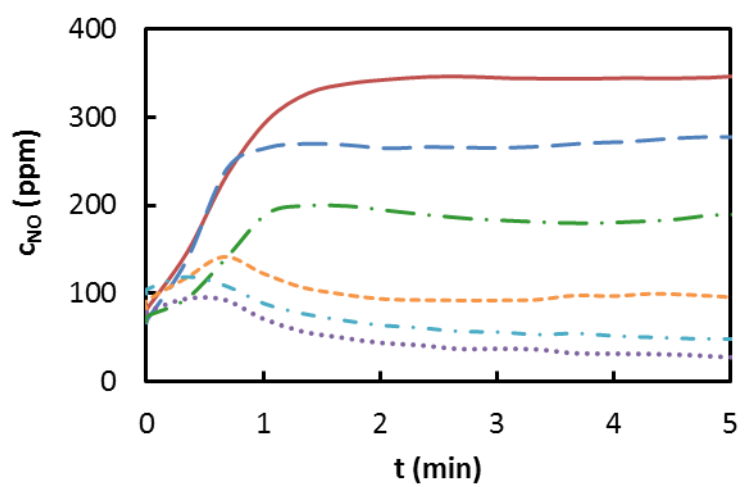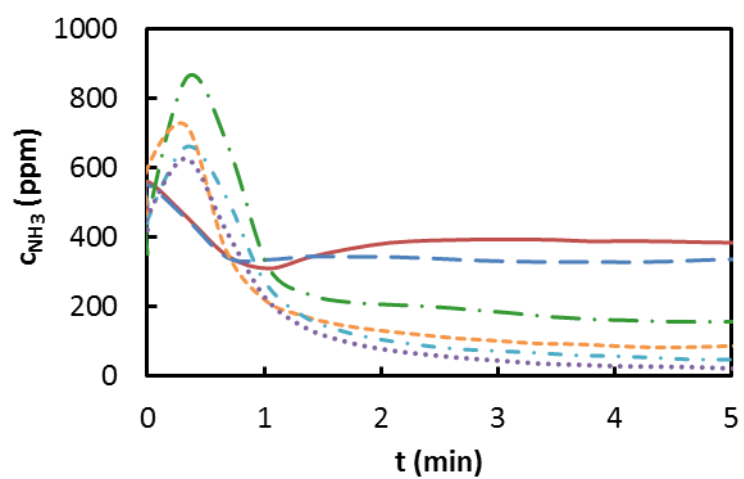
Mass spectrometer

TIC 02

TIC 01

PI 01

FIC 01

FIC 02

FIC 03

NH$_3$

NO

Air

4

5

6

7

8

1

Figure 2

3   a

4

5   b

6

7

1

Figure 3

3   a

4   b

5   c

1   **Figure 4**

2

3   a

4

5   b

6

7

1

Figure 5

2

3

4

5

6

1

Figure 6

3

4   a
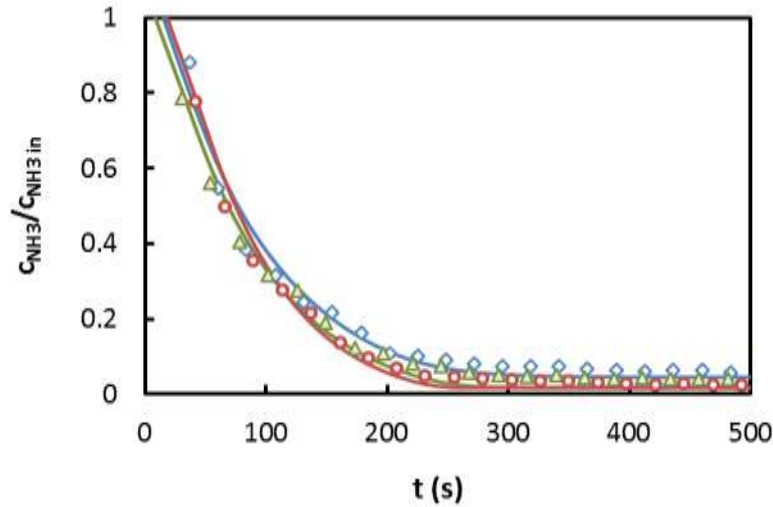

5   b

6

1

Figure 7

3

4   A

5

6   b

7

8

1
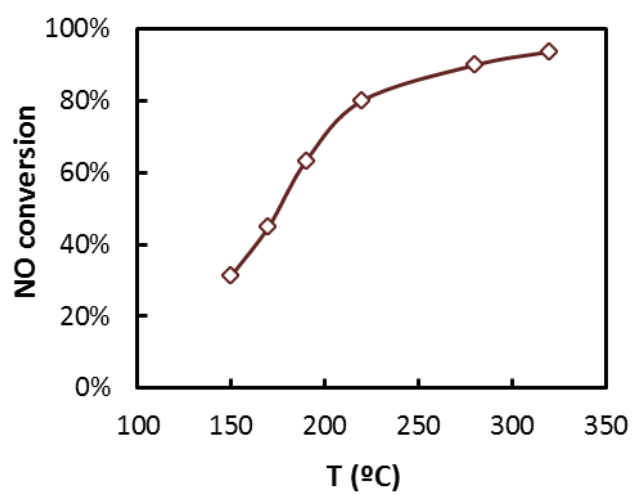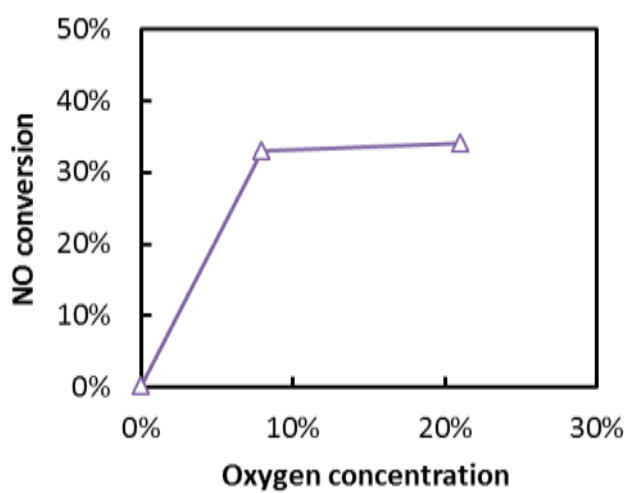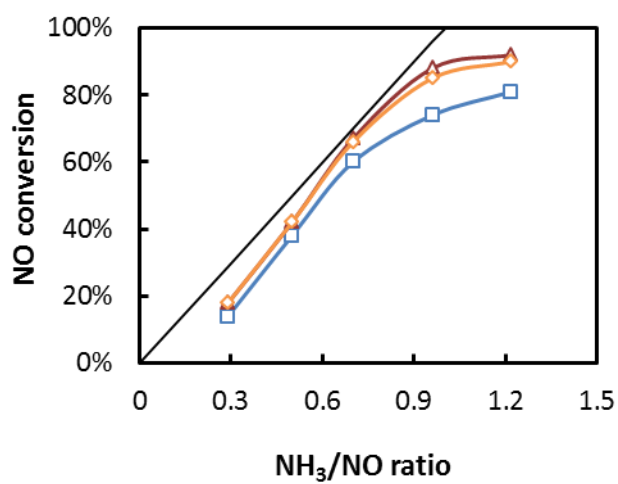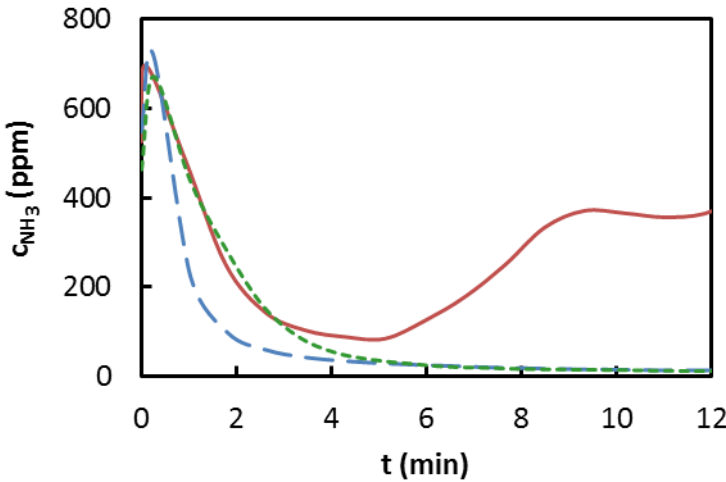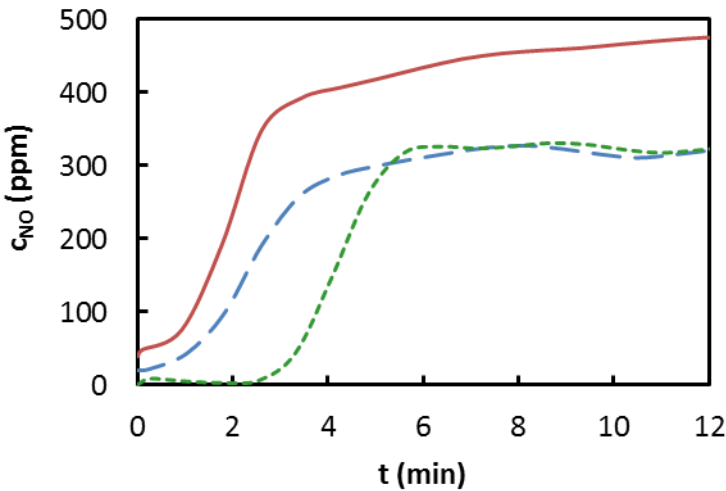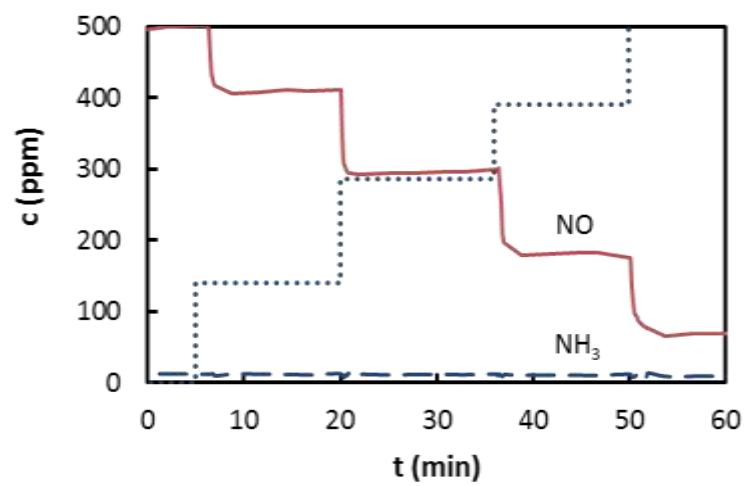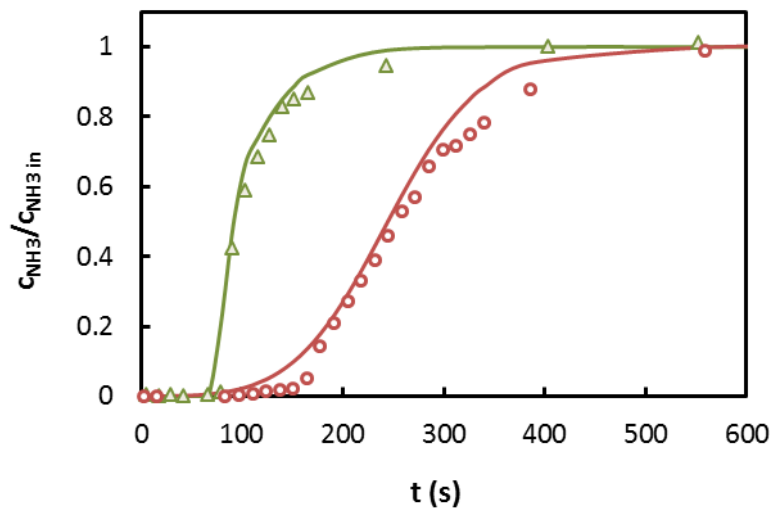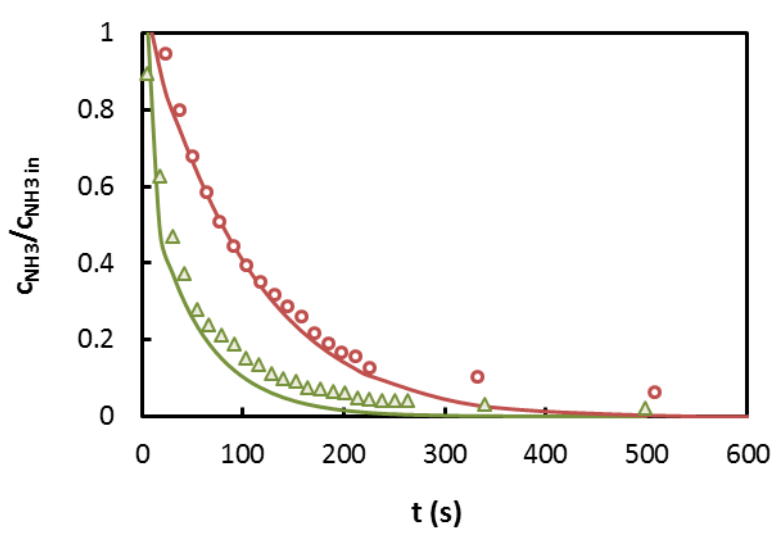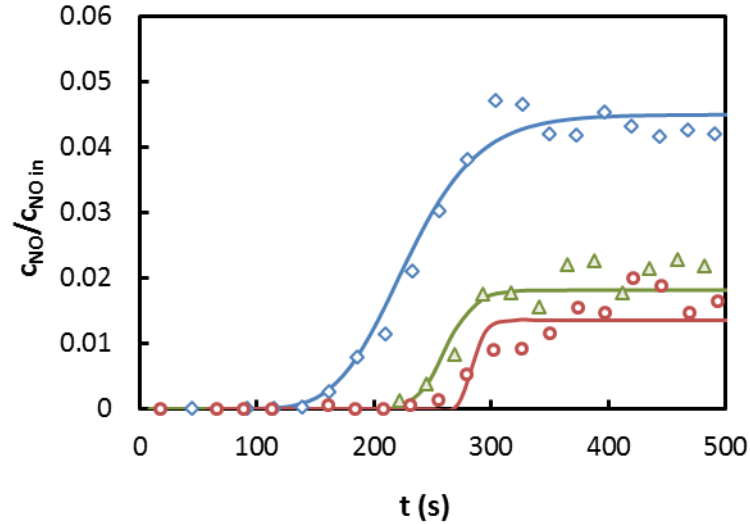
Figure 8

3

4
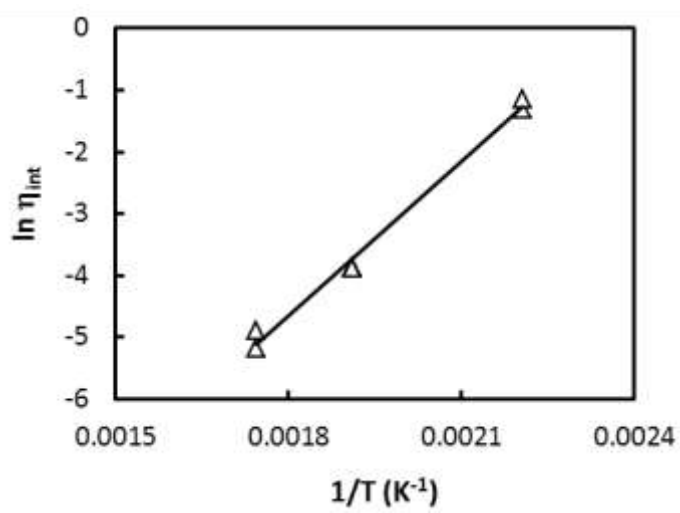
5

6

7

1

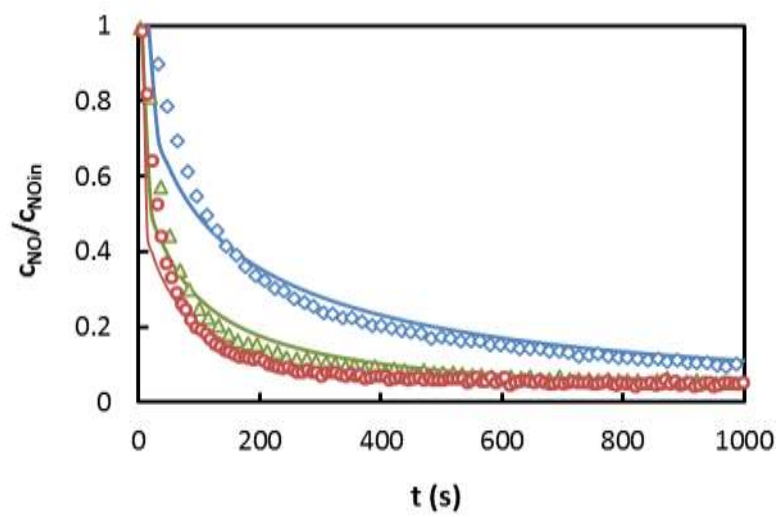2 **Figure 9**

3

4

5

6

1

2 **Figure 10**

3

4

5

6

7

1

List of tables

3

8

9

10

11

12

13

14

1 **Table 1**

2

Gas phase mass balances	Boundary conditions
Solid phase mass balance	Boundary conditions
Kinetic model	

3   A = NO, B = NH$_3$

4

5

1 **Table 2**

2

Gas phase mass balances	Boundary conditions

Solid phase mass balance	Boundary conditions

Interphase equations

Kinetic equations

3   A = NO, B = NH_3

4

5

6

1 **Table 3**

2

Kinetic parameters
0.113 mol NH_3 kg_{cat}^{-1}
2.75 m^3 mol^{-1} s^{-1}
0.0278 s^{-1} at 280ºC
9.8 kJ mol^{-1}
260 m^3 mol^{-1} s^{-1} at 280ºC
92.8 kJ mol^{-1}

3

4

5

References

1. Jin Y, Veiga MC and Kennes C, Bioprocesses for the removal of nitrogen oxides from polluted air. *Journal of Chemical Technology & Biotechnology* **80**: 483-494 (2005).
2. Roh SA, Jung SH, Jeong SM and Kim SD, Selective catalytic reduction by urea in a fluidized-bed reactor. *Journal of Chemical Technology & Biotechnology* **78**: 1104-1109 (2003).
3. Inger M, Wilk M, Parres-Esclapez S, Illán-Gómez MJ, Salinas-Martínez de Lecea C and Bueno-López A, Nitrous oxide decomposition in a real nitric acid plant gas stream with a RhOx/Ce0.9Pr0.1O2/alumina catalyst. *Journal of Chemical Technology & Biotechnology* **88**: 2233-2238 (2013).
4. Berger RJ, Kapteijn F, Moulijn JA, Marin GB, De Wilde J, Olea M, Chen D, Holmen A, Lietti L, Tronconi E and Schuurman Y, Dynamic methods for catalytic kinetics. *Applied Catalysis A: General* **342**: 3-28 (2008).
5. Nova I, Lietti L, Tronconi E and Forzatti P, Transient responce method applied to the kinetic analysis of the DeNOx-SCR reaction. *Chemical Engineering Science* **56**: 1229-1237 (2001).
6. Lietti L, Nova I, Camurri S, Tronconi E and Forzatti P, Dynamics of the SCR-DeNOx Reaction by the Transient-Response Method. *AIChE Journal* **43**: 2559-2570 (1997).
7. Shafeeyan MS, Wan Daud WMA and Shamiri A, A review of mathematical modeling of fixed-bed columns for carbon dioxide adsorption. *Chemical Engineering Research and Design* **92**: 961-988 (2014).
8. Zhibo X, Chunmei L, Dongxu G, Xinli Z and Kuihua H, Selective catalytic reduction of NOxwith NH3over iron-cerium mixed oxide catalyst: catalytic performance and characterization. *Journal of Chemical Technology & Biotechnology* **88**: 1258-1265 (2013).
9. Won W, Lee S and Lee KS, Modeling and parameter estimation for a fixed-bed adsorption process for CO2 capture using zeolite 13X. *Separation and Purification Technology* **85**: 120-129 (2012).
10. Tronconi E, Nova I, Ciardelli C, Chatterjee D, Brandl-Konrad B and Burkhardt T, Modelling of an SCR catalytic converter for diesel exhaust after treatment: Dynamic effects at low temperature. *Catalysis Today* **105**: 529-536 (2005).
11. Zhang, Chen and Shangguan, Low-temperature SCR of NO with propylene in excess oxygen over the Pt/TiO2 catalyst, in Catal Commun, pp. 1330-1333 (2009).
12. Liu F, Yu Y and He H, Environmentally-benign catalysts for the selective catalytic reduction of NOx from diesel engines: structure-activity relationship and reaction mechanism aspects. *Chemical Communications* (2014).
13. Roy S, Hegde MS and Madras G, Catalysis for NOx abatement. *Applied Energy* **86**: 2283-2297 (2009).
14. Kröcher O, Devadas M, Elsener M, Wokaun A, Söger N, Pfeifer M, Demel Y and Mussmann L, Investigation of the selective catalytic reduction of NO by NH3 on Fe-ZSM5 monolith catalysts. *Applied Catalysis B: Environmental* **66**: 208-216 (2006).
15. Iwamoto M and Hamada H, Removal of nitrogen monoxide from exhaust gases through novel catalytic processes. *Catalysis Today* **10**: 57-71 (1991).
16. Cheng X and Bi XT, A review of recent advances in selective catalytic NOx reduction reactor technologies. *Particuology*.
17. Odenbrand CUI, Bahamonde A, Avila P and Blanco J, Kinetic study of the selective reduction of nitric oxide over vanadia—tungsta—titania/sepiolite catalyst. *Applied Catalysis B: Environmental* **5**: 117-131 (1994).
18. Koebel M and Elsener M, Selective catalytic reduction of NO over commercial DeNOx-catalysts: experimental determination of kinetic and thermodynamic parameters. *Chemical Engineering Science* **53**: 657-669 (1998).

19. Tronconi E, Lietti L, Forzatti P and Malloggi S, Experimental and theoretical investigation of the dynamics of the SCR - DeNOx reaction. *Chemical Engineering Science* **51**: 2965-2970 (1996).

20. Pinaeva LG, Suknev AP, Budneva AA, Paukshtis EA and Bal'zhinimaev BS, On the role of oxygen in the reaction of NO reduction by NH3 over monolayer V2O5⊡TiO2 catalyst. *Journal of Molecular Catalysis A: Chemical* **112**: 115-124 (1996).

21. Busca G, Larrubia MA, Arrighi L and Ramis G, Catalytic abatement of NOx: Chemical and mechanistic aspects. *Catalysis Today* **107–108**: 139-148 (2005).

22. Busca G, Lietti L, Ramis G and Berti F, Chemical and mechanistic aspects of the selective catalytic reduction of NOx by ammonia over oxide catalysts: A review. *Applied Catalysis B: Environmental* **18**: 1-36 (1998).

23. Lei Z, Han B, Yang K and Chen B, Influence of H2O on the low-temperature NH3-SCR of NO over V2O5/AC catalyst: An experimental and modeling study. *Chemical Engineering Journal* **215–216**: 651-657 (2013).

24. Inomata M, Miyamoto A and Murakami Y, Mechanism of the reaction of NO and NH3 on vanadium oxide catalyst in the presence of oxygen under the dilute gas condition. *Journal of Catalysis* **62**: 140-148 (1980).

25. Ramis G, Busca G, Bregani F and Forzatti* P, Fourier transform-infrared study of the adsorption and coadsorption of nitric oxide, nitrogen dioxide and ammonia on vanadia-titania and mechanism of selective catalytic reduction. *Applied Catalysis* **64**: 259-278 (1990).

26. Tufano V and Turco M, Kinetic modelling of nitric oxide reduction over a high-surface area V2O5-TiO2 catalyst. *Applied Catalysis B: Environmental* **2**: 9-26 (1993).

27. Topsoe NY, Topsoe H and Dumesic JA, Vanadia/Titania Catalysts for Selective Catalytic Reduction (SCR) of Nitric-Oxide by Ammonia: I. Combined Temperature-Programmed in-Situ FTIR and On-line Mass-Spectroscopy Studies. *Journal of Catalysis* **151**: 226-240 (1995).

28. Topsoe NY, Dumesic JA and Topsoe H, Vanadia-Titania Catalysts for Selective Catalytic Reduction of Nitric-Oxide by Ammonia: II. Studies of Active Sites and Formulation of Catalytic Cycles. *Journal of Catalysis* **151**: 241-252 (1995).

29. Marin P, Fissore D, Barresi AA and Ordonez S, Simulation of an industrial-scale process for the SCR of NOx based on the loop reactor concept. *Chemical Engineering and Processing* **48**: 311-320 (2009).

30. Hayes RE and Kolaczkowski ST, Introduction to catalytic combustion. Gordon and Breach Science Publishers, Amsterdam (1997).

31. Marín P, Ordóñez S and Díez FV, Monoliths as suitable catalysts for reverse-flow combustors: modeling and experimental validation. *AIChE Journal* **56**: 3162-3173 (2010).

32. Marin P, Ordonez S and Diez FV, Systematic study of the performance of a reverse flow reactor for the treatment of lean hydrocarbon emissions. *Journal of Chemical Technology and Biotechnology* **84**: 1292-1302 (2009).

33. Chen C-T and Tan W-L, Mathematical modeling, optimal design and control of an SCR reactor for NOx removal. *Journal of the Taiwan Institute of Chemical Engineers* **43**: 409-419 (2012).

34. Heck RM, Catalytic abatement of nitrogen oxides–stationary applications. *Catalysis Today* **53**: 519-523 (1999).

35. Svachula J, Ferlazzo N, Forzatti P, Tronconi E and Bregani F, Selective reduction of NOx by NH3 over honeycomb DeNOxing catalysts. *Industrial and Engineering Chemistry Research* **32**: 1053-1060 (1993).